


D. BANERJEE  
J. RYBCZYNSKI  
J.Y. HUANG  
D.Z. WANG  
K. KEMPA  
Z.F. REN 

# Large hexagonal arrays of aligned ZnO nanorods

Department of Physics, Boston College, Chestnut Hill, Massachusetts 02467, USA

Received: 5 July 2004/Accepted: 21 October 2004

Published online: 15 December 2004 • © Springer-Verlag 2004

**ABSTRACT** Large-scale truly periodic arrays of vertically aligned zinc oxide nanorods were grown on pre-patterned and pre-annealed gold dots on *a*-plane sapphire substrates via the vapor–liquid–solid mechanism. Periodic arrays of triangular gold islands were first patterned on the *a*-plane sapphire substrates by the nanosphere self-assembly technique. Zinc has been found to be an effective interfacial modifier between gold and sapphire to form single catalytic dots from triangular islands. The successful fabrication of zinc oxide nanowires in truly periodic arrays opens up the possibility of achieving enhanced room-temperature ultraviolet lasing and photonic crystal based devices and sensors.

PACS 81.07.Bc; 81.10.-h; 81.16.Nd

## 1 Introduction

Demonstration of room-temperature ultraviolet (UV) lasing from vertically aligned arrays of zinc oxide (ZnO) nanorods [1] initiated a great interest in fabrication of ZnO nanostructures and their applications in various optoelectronic devices [2–4]. ZnO is a wide band gap (3.37 eV) semiconductor with a high exciton binding energy of 60 meV, substantially higher than ZnSe (22 meV) and GaN (25 meV). Compared to other wide band gap semiconductors (ZnSe, GaN, SiC, etc.), ZnO has properties such as higher chemical and thermal stability, higher radiation hardness, and lower growth temperature. ZnO thin films and particles have been extensively used for blue optoelectronic applications, surface acoustic wave devices, optical waveguides, and transparent conductive thin films [5–13].

In the last few years, carbothermal-based vapor phase growth has been well studied to achieve control over selective-area growth [14, 15] as well as freestanding, large-quantity production of ZnO nanorods [16, 17]. Arrays of vertically aligned ZnO nanorods can be grown epitaxially on *a*-plane sapphire or (111) MgO substrates via the vapor–liquid–solid (VLS) mechanism from either a catalytic thin film or nanoparticles [18]. Recently, growth of hexagonal-like arrays of ZnO nanorods was reported [4]. However, the periodicity

was not truly hexagonal since each site contained several nanorods [4]. Therefore, it is still a challenge to grow a truly periodically aligned ZnO nanorod array for various device applications. The difficulty is to avoid the diffusion and migration of the catalyst dots at high processing temperature, which destroys the pre-patterned periodicity.

Here we report a success in achieving large truly periodic arrays of ZnO nanorods on transparent *a*-plane sapphire substrates using the nanosphere self-assembly technique [19–22]. This technique opens up a variety of possibilities of using such arrays as photonic band gap crystals, negative index of refraction media, super-lenses, and super-strong room-temperature UV lasers.

## 2 Experimental

The *a*-plane sapphire substrates were patterned with periodic triangular gold (Au) islands by nanosphere self-assembly. Briefly, a monolayer of self-assembled submicron polystyrene (PS) spheres was formed on a water surface and was then transferred to the *a*-plane sapphire substrate, followed by an e-beam evaporation of a 1–5 nm Au film. The spheres were then removed via ultrasonication in tetrahydrofuran for 10 min to yield periodic triangular Au islands. Size and spacing of the Au islands were tuned by varying the size of the PS spheres. In our study microspheres of 440 and 540 nm were used. These masks can be as large as  $10 \times 10 \text{ cm}^2$ .

In order to reduce each triangular Au island into a single dot, we used a two-step annealing procedure to treat the Au islands. First, ZnO powder (Alfa Aesar, 99.9%) and graphite powder (Alfa Aesar, 99.9%) were mixed in 1:1 weight ratio and placed in one end of a quartz boat as the source. In the same boat the *a*-plane sapphire substrate with the Au pattern was placed at 6–7 cm away from the source down the air flow. The entire assembly was inserted into a horizontal tube furnace and heated to 850 °C at the source and 600 °C at the substrates for 30 min with constant flowing Ar gas (50 sccm) to maintain a pressure of 1.5 Torr, then cooled to 550 °C, and taken out. Second, the substrates were put back into the boat with a new source at the same distance of 6–7 cm and heated to 950 °C at the source and 720 °C at the substrates for 15 min, then cooled to 200 °C, and taken out. For the growth of the nanorods, a new source mixture and the two-step annealed substrates were arranged in the same way as in the first-step annealing, heated to 850–900 °C at the source and

600–650 °C at the substrates with a constant flow (50 sccm) of argon gas mixed with 2% of oxygen introduced to maintain a pressure of 1.5 Torr. The morphology and the structural characterization were carried out by scanning electron microscopy (SEM, JEOL-6340F) and transmission electron microscopy (TEM, JEOL-2010F).

### 3 Results and discussion

Figure 1a and b show the atomic force microscopic (AFM) and SEM images of the PS monolayer on sapphire, respectively. Figure 1c shows the SEM image of the hexagonal pattern of the triangular Au islands after removal of PS. Figure 1d shows the formation of the multiple particles from each triangular Au island when treated in oxygen. Figure 1e shows the corresponding growth of ZnO nanorods from the same Au particles as shown in Fig. 1d, which is consistent with the previous study [22]. In the Au–sapphire system, at an elevated temperature the adhesion of Au to sapphire increases significantly in an oxygen-rich atmosphere. High interfacial adhesion causes fracture of an Au thin film leading to formation of several spherical droplets on each original Au island.

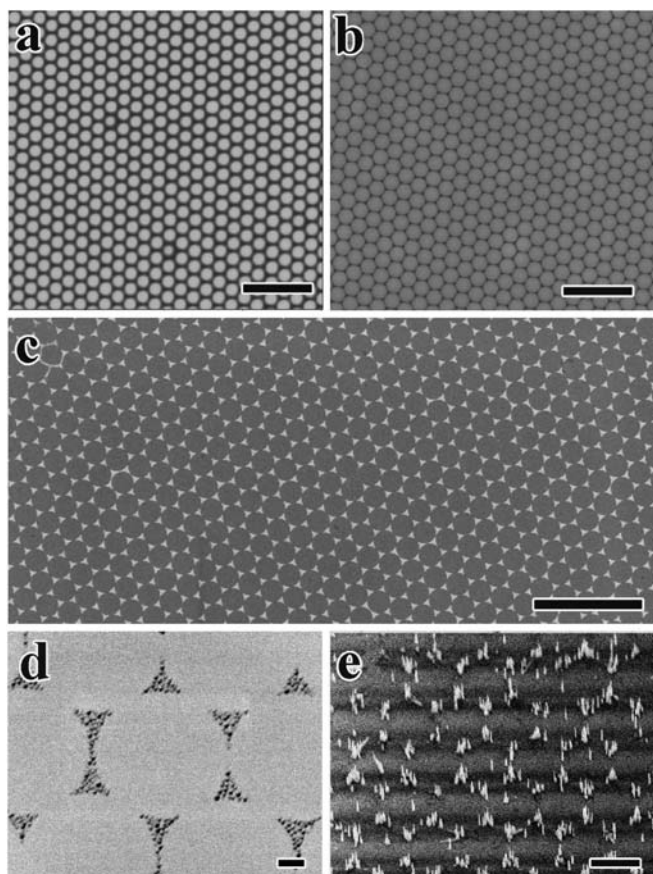


**FIGURE 1** Nanosphere self-assembly and nanorod growth. **a** and **b** AFM and SEM micrographs of the mask prepared by PS spheres, **c** SEM image of the triangular Au dots after removal of the mask, **d** SEM image of the substrate after heat treatment without any source material, to show the formation of multiple small Au dots on each original Au site, **e** aligned growth of ZnO nanorods on these substrates, where each site consists of several nanorods. Scale bars: **a**, **b**, and **c** 5  $\mu\text{m}$ , **d** 100 nm, **e** 1  $\mu\text{m}$

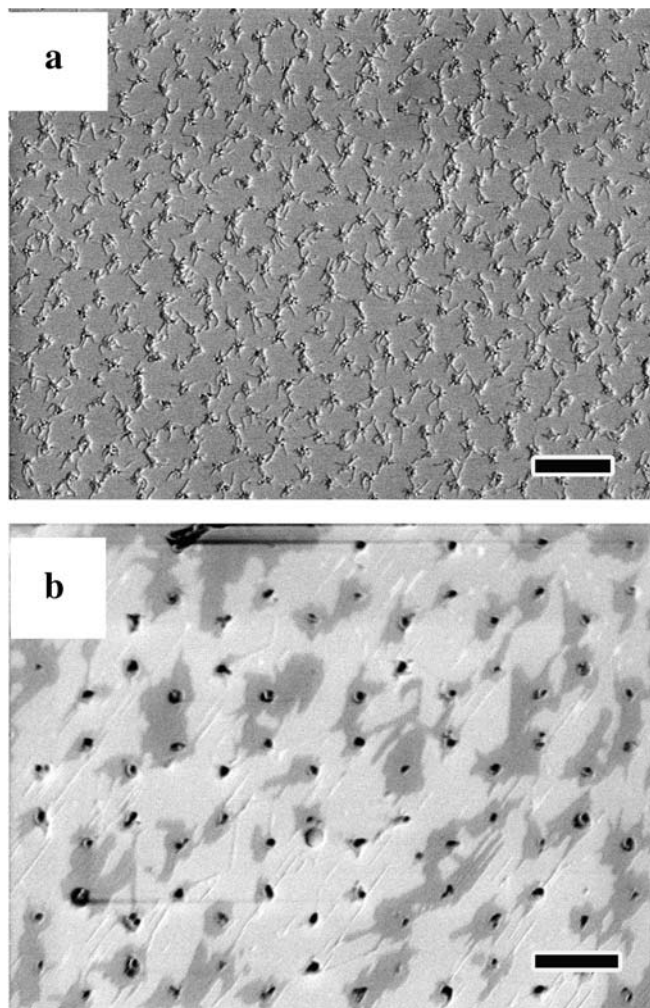


**FIGURE 2** SEM images of the patterned substrates after annealing. **a** After the first step of annealing, **b** after the second step of annealing. Scale bars: **a** 1  $\mu\text{m}$ , **b** 500 nm

We avoided the formation of multiple small Au particles by the two-step annealing procedure described above. In the first step, the catalytic sites absorb the incoming Zn vapor without breaking into multiple small particles as shown in Fig. 2. Figure 2a shows the top view of the SEM image of the substrate after such treatment. It is clear that the triangular Au islands shrink into single dots. We believe that it is because semi-saturated Au–Zn alloy is less adhesive to the sapphire substrate than pure Au. However, very thin ZnO nanorods can be seen on each site due to the presence of a trace amount of oxygen from the source. To eliminate the growth of these thin ZnO nanorods, the second step was used. Figure 2b shows a sapphire substrate after the two steps of annealing, where each site contains either one or at most two Zn-rich Au nanoparticles.

Figure 3 shows the SEM micrographs of the large periodic array of ZnO nanorods. Figure 3a shows the array viewed at 20°. The typical length of the nanorods varies from a few hundred nanometers to 2  $\mu\text{m}$  and the diameter varies from 20 to 40 nm. Nanorods with a length of more than 2  $\mu\text{m}$  have a tendency to merge with a neighboring rod at the tip, as shown in Fig. 3b. Figure 3c shows the array of shorter nanorods,

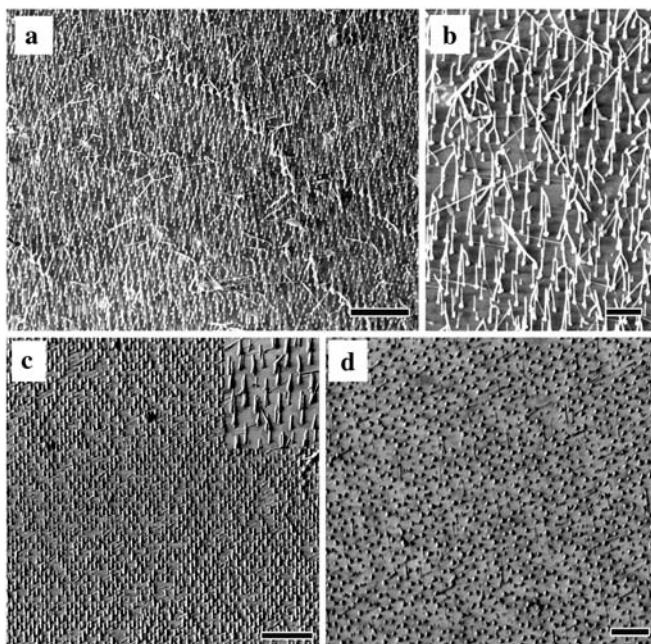


**FIGURE 3** SEM images of the periodic arrays of aligned ZnO nanorods: **a** and **b** the longer (2–3  $\mu\text{m}$ ) nanorod arrays, **c** shorter nanorods with a closer view of the periodic arrangement in the *inset*, **d** top view of these arrays. Scale bars: **a** 5  $\mu\text{m}$ , **b** 1  $\mu\text{m}$ , **c** 5  $\mu\text{m}$ , **d** 1  $\mu\text{m}$

with occasionally missing sites. Figure 3d is a top view of the arrays as shown in Fig. 3c. Obvious periodicity of the hexagonal arrangement of the nanorods' locations can be noticed. Most of the sites are a single vertical nanorod but, in some places, two or even three nanorods were formed. The length and diameter of the nanorods depend on the experimental conditions such as thickness of the Au film, temperature, and growth time.

To demonstrate the effect of external oxygen partial pressure on alignment, arrays were also grown on a very thick (about 35 nm) Au pattern without any external oxygen flow during the growth. We observed formation of very small and poorly aligned individual nanorods as shown in Fig. 4, although the periodic arrangement was intact. This further proves that the multiple growths of nanorods are caused by the excessive oxygen partial pressure. Figure 5 presents TEM im-

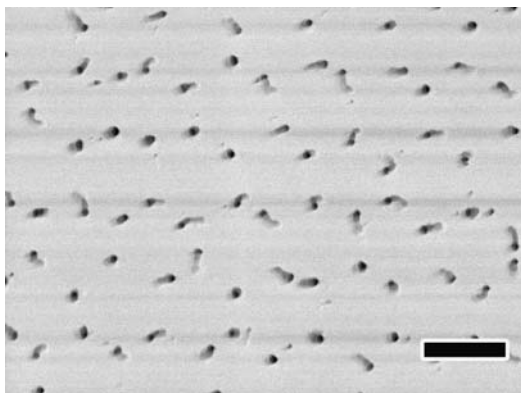


**FIGURE 4** SEM image of the periodic arrays of semi-aligned ZnO nanorods obtained without oxygen gas flowing during growth. Scale bars: 500 nm

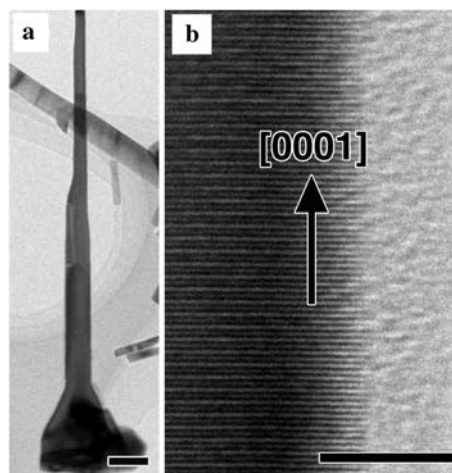


**FIGURE 5** **a** TEM image of a single ZnO nanorod, **b** high-resolution TEM image of the rod to show the growth direction and good crystallinity. Scale bars: **a** 50 nm, **b** 5 nm

ages of a single nanorod. From Fig. 5a, it is clear that a bulge was formed in the bottom. Figure 5b shows that the wire-growth direction is [0001], and there is a thin amorphous graphite layer on the surface, which could be removed easily by oxidation [16, 17].

In summary, we have demonstrated an effective and low-cost method to fabricate ZnO nanorods in large truly periodic arrays on *a*-plane sapphire substrates. Periodic Au islands as catalyst were patterned on a sapphire substrate by nanosphere self-assembly. In contrast to the previous report [4], we managed to avoid multiple growth on each catalytic site by a two-step annealing procedure of the Au islands to form Au dots due to the reduction of adhesion of Au–Zn alloy with sapphire. Site density and length of the nanorods can be well controlled by tuning various experimental parameters. Positioning of ZnO nanorods in a periodic array may find numerous applications in high-performance optoelectronic, sensing, and photonic crystal based devices.

**ACKNOWLEDGEMENTS** The work performed by Z.F. Ren is supported by the DOE under Grant No. DE-FG02-00ER45805, and the work done by D. Banerjee is supported by the US Army Natick Soldier Systems Center under Grant No. DAAD16-03-C-0052.

## REFERENCES

- 1 M. Huang, S. Mao, H. Feick, H. Yan, Y. Wu, H. Kind, E. Weber, R. Russo, P. Yang: *Science* **292**, 1897 (2001)
- 2 (a) H. Yan, J. Justin, M. Law, R. Saykally, P. Yang: *Adv. Mater.* **15**, 1907 (2003); (b) H. Kind, H. Yan, M. Law, B. Messer, P. Yang: *Adv. Mater.* **14**, 158 (2003); (c) J.C. Johnson, K.P. Knutsen, H.Q. Yan, M. Law, Y.F. Zhang, P.D. Yang, R.J. Saykally: *Nano Lett.* **4**, 197 (2004)
- 3 C.H. Liu, J.A. Zapfen, Y. Yao, X.M. Meng, C.S. Lee, S.S. Fan, Y. Lifshitz, S.T. Lee: *Adv. Mater.* **15**, 838 (2003)
- 4 X. Wang, C.J. Summers, Z.L. Wang: *Nano Lett.* **4**, 423 (2004)
- 5 E.M. Wong, P.C. Searson: *Appl. Phys. Lett.* **74**, 2939 (1999)
- 6 Y. Nakanishi, A. Miyake, H. Kominami, T. Aoki, Y. Hatanaka, G. Shimaoka: *Appl. Surf. Sci.* **142**, 233 (1999)
- 7 Y. Li, G.W. Meng, L.D. Zhang, F. Philipp: *Appl. Phys. Lett.* **76**, 2011 (2000)
- 8 D.C. Look: *Mater. Sci. Eng. B* **80**, 383 (2001)
- 9 E.L. Paradis, A.J. Shuskus: *Thin Solid Films* **83**, 131 (1976)
- 10 F.M.C. Van De Pol: *Ceram. Bull.* **69**, 1959 (1990)

- 11 A.J. Freeman, K.R. Poepelmeier, T.O. Mason, R.P.H. Chang, T.J. Marks: *Mater. Res. Soc. Bull.* **25**, 45 (2000)
- 12 D.S. Ginley, C. Bright: *Mater. Res. Soc. Bull.* **25**, 15 (2000)
- 13 M. Kadota: *Jpn. J. Appl. Phys.* **36**, 3076 (1997)
- 14 B.D. Yao, Y.F. Chan, N. Wang: *Appl. Phys. Lett.* **81**, 4 (2002)
- 15 M.H. Huang, Y. Wu, H. Feick, N. Tran, E. Weber, P. Yang: *Adv. Mater.* **13**, 113 (2001)
- 16 D. Banerjee, J.Y. Lao, D.Z. Wang, J.Y. Huang, Z.F. Ren, D. Steeves, B. Kimball, M. Sennett: *Appl. Phys. Lett.* **83**, 2061 (2003)
- 17 D. Banerjee, J.Y. Lao, D.Z. Wang, J.Y. Huang, D. Steeves, B. Kimball, Z.F. Ren: *Nanotechnology* **15**, 404 (2004)
- 18 P. Yang, H. Yan, S. Mao, R. Russo, J. Johnson, R. Saykally, N. Morris, J. Pham, R. He, H.J. Choi: *Adv. Funct. Mater.* **12**, 323 (2002)
- 19 K. Kempa, B. Kimball, J. Rybczynski, Z.P. Huang, P.F. Wu, D. Steeves, M. Sennett, M. Giersig, D.V.G.L.N. Rao, D.L. Carnahan, D.Z. Wang, J.Y. Lao, W.Z. Li, Z.F. Ren: *Nano Lett.* **3**, 13 (2003)
- 20 J. Rybczynski, U. Ebels, M. Giersig: *Colloid Surf. A – Physicochem. Eng. Aspects* **219**, 1 (2003)
- 21 Y. Wang, J. Rybczynski, D.Z. Wang, W.Z. Li, B. Kimball, K. Kempa, Z.F. Ren: *Appl. Phys. Lett.* **85**, 4741 (2004)
- 22 D.M. Lipkin, D.R. Clarke, A.G. Evans: *Acta Mater.* **46**, 4835 (1998)